PCCP

RSC Publishing

PAPER

Strong intramolecular charge transfer emission in benzobisoxazole cruciforms: solvatochromic dyes as polarity indicators†

Cite this: *Phys. Chem. Chem. Phys.*, 2013, **15**, 18023

Virginia Martínez-Martínez,*[a] Jaebum Lim,[b] Jorge Bañuelos,[a] Iñigo López-Arbeloa[a] and Ognjen Š. Miljanić*[b]

Received 19th August 2013,
Accepted 6th September 2013

DOI: 10.1039/c3cp53527d

www.rsc.org/pccp

A photophysical study was carried out on a series of nine X-shaped cross-conjugated compounds based on the benzobisoxazole nucleus. These ''molecular cruciforms'' were terminally substituted with electron-rich 4-(*N*,*N*-dimethylamino)phenyl, electron-neutral phenyl or electron-poor 4-pyridyl groups. Intramolecular charge transfer (ICT) transitions in molecular cruciforms were shown to be activated to a different extent by the combinations of these substituents located in different positions along vertical and/or horizontal axes of the molecules, showing strong emission throughout the visible spectrum. The high fluorescence efficiency and bathochromic shifts associated with the increasing polarity of the solvent make these cruciforms interesting candidates for use as fluorescence polarity indicators operating in a broad solvatochromic range.

Introduction

Molecular cruciforms are X-shaped chromophores constructed by two perpendicular π-conjugated arms intersecting at a central aromatic core.[1] With appropriate substitution, these compounds localize their frontier molecular orbitals (FMOs) on different portions of the molecule, so that the electron-rich arm bears the bulk of the highest occupied molecular orbital (HOMO) density, while the lowest unoccupied molecular orbital (LUMO) predominantly resides along the electron-poor arm of the molecule. This spatial isolation of FMOs makes molecular cruciforms superb candidates for a variety of optoelectronic applications, as their FMOs can be independently addressed and thus HOMO–LUMO gaps can be predictably modulated. This property has been utilized by Haley,[2] Bunz[1a,3] and Miljanić[4] groups to develop molecular cruciforms into fluorescent sensors for carboxylic acids,[1a,2c,g,3e,4c] metals,[3m,q] boronic acids,[4c] amines,[3b,c,j,4b] small organic and inorganic anions,[3l,4a,b,g] and phenols.[4c]

Installation of electron-donating and/or electron-withdrawing groups onto the cruciform structure can lead to different charge-transfer pathways, which in turn allow the tuning of the emission colour. Several spectroscopic studies have been performed on diverse cruciform families with different donor–acceptor patterns.[1a,2g,3d,f,s] However, upon donor–acceptor substitution, the resultant quantum yield usually drops to under 20%. This is a typical effect for charge transfer (CT) states because the smaller HOMO–LUMO gaps allow for more favourable non-radiative relaxation mechanisms. The imposition of rigidity to the structure in this case would help to increase the fluorescence rate.

In this work, we describe the exhaustive spectroscopic characterization of a class of nine fully conjugated benzobisoxazole cruciforms **1–9** (Fig. 1), previously synthesized by the Miljanić group.[4d] Within this compound class, substituents on the vertical and horizontal axes have been varied pairwise between electron-neutral phenyl, electron-rich 4-(*N*,*N*-dimethylamino)phenyl and electron-poor 4-pyridyl groups, with the intention of observing how these changes affected the optical properties of these molecules. Previously, benzobisoxazole cruciforms have been proven to be excellent fluorophore sensors, capable of distinguishing structurally closely related Brønsted and Lewis acids.[4c,d] In self-assembled complexes with non-fluorescent boronic acids, benzobisoxazole cruciforms were also shown to be competent sensors for Lewis bases,[4b,c] as evidenced by the drastic changes in the emission colours. Herein, we report a detailed photophysical study of these nine cruciform molecules in several different solvents. This study reveals that cruciforms substituted with electron-rich 4-(*N*,*N*-dimethylamino)phenyl groups have a pronounced

[a] *Departamento de Química Física, Universidad del País Vasco, UPV/EHU, Apartado 644, 48080 Bilbao, Spain. E-mail: virginia.martinez@ehu.edu; Fax: +34 946013500; Tel: +34 946015384*

[b] *Department of Chemistry, University of Houston, 112 Fleming Building, Houston, TX 77204-5003, USA. E-mail: miljanic@uh.edu; Fax: +1-713-743-2709; Tel: +1-832-842-8827*

† Electronic supplementary information (ESI) available: HOMO and LUMO contour maps, additional spectra and photophysical parameters. See DOI: 10.1039/c3cp53527d

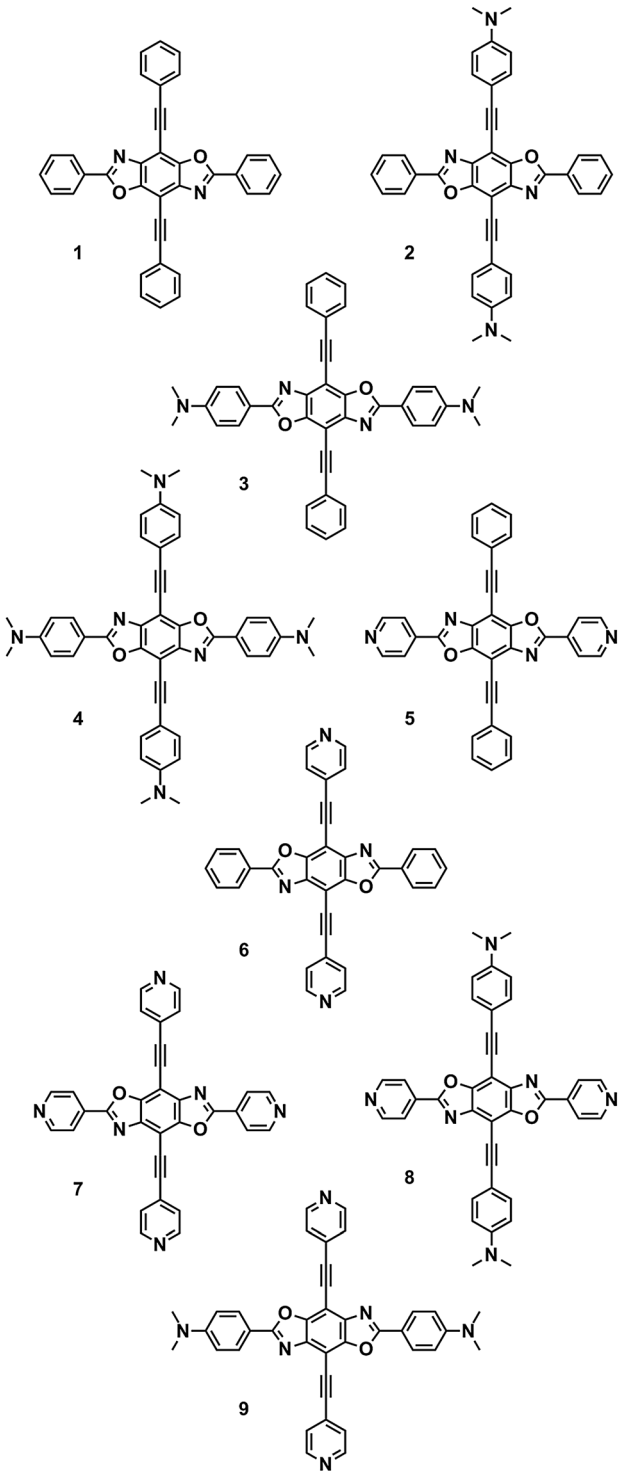

Fig. 1 Cruciform-shaped benzobisoxazole fluorophores **1–9** discussed in this study.

intramolecular charge transfer (ICT) band, characterized by high solvatochromism and quantum yields that exceed 50% even in polar solvents. The high fluorescence efficiency and strong bathochromic shifts associated with increasing solvent polarity make these cruciforms potentially useful as fluorescent polarity sensors.

Experimental

The photophysical properties were measured in dilute (approx. 2×10^{-6} M) solutions of **1–9**, prepared by adding the corresponding solvent to the residue from the adequate amount of a concentrated stock solution in dichloromethane (DCM), after vacuum evaporation of this solvent. UV-Vis absorption and fluorescence spectra were recorded on a Varian model CARY 4E spectrophotometer and a SPEX Fluorolog 3-22 spectrofluorimeter, respectively. The fluorescence spectra were corrected from the wavelength dependence of the detector sensitivity. Fluorescence quantum yields (ϕ) were obtained using several reference solutions: (*a*) aqueous solution of quinine sulfate in 0.1N H_2SO_4 ($\phi^r = 0.54$), (*b*) ethanolic solution of coumarin 152 ($\phi^r = 0.19$) and (*c*) ethanolic solution of BODIPY 597 ($\phi^r = 0.43$).

Radiative decay curves were registered with the time-correlated single-photon counting technique (Edinburgh Instruments, model FL920) using a microchannel plate detector (Hamamatsu C4878) with a picosecond ($\sim$20 ps) time resolution. Fluorescence emission was monitored at the maximum emission wavelength after excitation at 370 nm by means of a diode laser (PicoQuant, model LDH) with 150 ps FWHM pulses. The fluorescence lifetime (τ) was obtained from the slope after the deconvolution of the instrumental response signal from the recorded decay curves by means of an iterative method. The goodness of the exponential fit was controlled by statistical parameters (chi-square, Durbin–Watson and the analysis of the residuals). The radiative (k_{fl}) and non-radiative deactivation (k_{nr}) rate constants were calculated to be $k_{fl} = \phi/\tau$ and $k_{nr} = (1 - \phi)/\tau$, respectively.

Results and discussion

We first investigated the optical properties of cruciform **1** in different solvents. Cruciform **1** is substituted with electron-neutral phenyl groups along both its horizontal and vertical axes. The molecular orbitals of **1** reveal a strong electronic rearrangement upon excitation from the vertical axis to the horizontal axis (see HOMO–LUMO contour maps in the ESI†), which is typical of ICT transitions. However, its photophysical properties practically do not change in different media. The UV/Vis absorption and fluorescence bands of cruciform **1** (Fig. 2) are centered at around 366 nm and 400 nm, respectively. Quantum yields of $\phi = 0.75$ and fluorescence lifetimes values of around 1.4 ns derived from the radiative decay curves (analyzed as monoexponential, Table 1 and Table S1 in the ESI†) are similar in apolar, polar and protic solvents. Therefore, the electronic transition in compound **1** is attributed to a locally excited (LE) state, and not to an ICT transition. Indeed, the vibrational structure in the fluorescence spectra is observed in most solvents, with the exception of 2,2,2-trifluoroethanol (F3Et), which—as the protic solvent with the highest acidity in the series[5]—likely engages in solute–solvent interactions with the heteroatoms of the oxazole ring. In polar protic solvents such as ethanol (EtOH) or F3Et, these specific interactions provoke a slight increase in the Stokes shift and fluorescence lifetimes, together with a small decrease in radiative deactivation rate constants (k_{fl}) and fluorescence quantum yields.

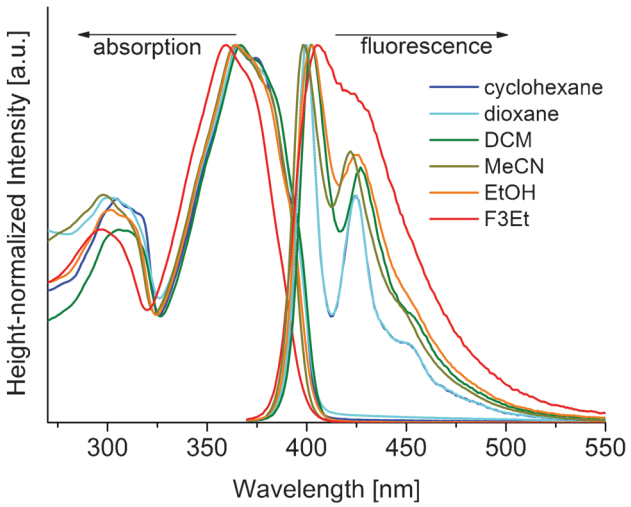

Fig. 2 Absorption and emission spectra of compound **1** in different solvents.

Table 1 Photophysical parameters of representative cruciforms in different solvents: absorption (λ_{abs}, in nm) and fluorescence wavelengths (λ_{fl}, in nm), fluorescence quantum yield (ϕ_{fl}), lifetime (τ, in ns) and radiative (k_{fl}, in $\times 10^8$ s^{-1}) and nonradiative deactivation (k_{nr}, in $\times 10^8$ s^{-1}) rate constants

	Solvent	λ_{abs}	λ_{fl}	ϕ_{fl}	τ (ns)	k_{fl}	k_{nr}
1	DCM	367	402.5	0.77	1.40	5.38	1.61
2	*c*-Hex[a]	423/373	460	0.70[a]	1.53	4.58	1.96
2	Diox	428/375	494	0.82	2.20	3.78	0.83
2	DCM	441/374	529	0.79	2.85	2.77	0.74
2	EtOH	434/372	585	0.38	1.5(20)/2.90(80)	1.33	2.18
2	F3Et[a]	422/363	630	0.01	0.1(55)/0.7(45)	—	—
2	MECN	438/371	605	0.26	3.27	0.80	2.26
3	*c*-Hex[a]	431/378	445	—	1.30	—	—
3	Diox	438/377	474.5	0.78	1.70	4.64	1.31
3	DCM	443/377	497.5	0.75	2.00	3.75	1.25
3	EtOH[a]	440/376	508	0.63	0.2(15)/2.4(85)	2.63	1.54
3	F3Et[a]	435/371	526	0.53	0.5(13)/3.0(87)	1.77	1.57
3	MECN	440/374	546	0.71	3.26	2.18	0.89
4	*c*-Hex[a]	410	440	[a]	0.5(28)/1.1(72)	—	—
4	Diox	413	458	0.69	0.65(20)/1.4(80)	4.89	2.20
4	DCM	421	483	0.81	0.9(22)/1.8(78)	4.45	1.04
4	EtOH	421	534	0.44	1.8(25)/2.9(75)	1.64	2.09
4	MECN	421	547	0.44	1.7(19)/3.3(81)	1.32	1.68
8	*c*-Hex[a]	454/350	498	0.67[a]	2.65	2.53	1.24
8	Diox	452/342	514	0.69	2.66	2.59	1.16
8	DCM	469/351	606	0.58	3.78	1.27	1.38
9	*c*-Hex[a]	449/350	471	—	1.78	—	—
9	Diox	452/344	514	0.73	2.64	2.76	1.02
9	DCM	459/347	547	0.81	3.50	2.31	0.54
9	EtOH	461/347	594	0.18	1.75	1.03	4.69
9	MECN	456/344	615	0.24	2.38	1.01	3.19

[a] Compound not fully soluble (higher experimental error in the calculation of ϕ due to the low absorbance at the excitation wavelength).

The presence of the strongly electron-donating 4-(*N*,*N*-dimethylamino)phenyl group on the vertical axis of compound **2** enhances the inherent donor character of this axis and results overall in a significantly higher HOMO orbital density along the vertical arm of the molecule. The effect of the strongly electron-donating substituents of **2** is reflected in its ionization potential of −7.78 eV (relative to −8.30 eV in **1**, see the ESI†). Thus, in this compound, a clear ICT transition should be expected. Indeed, in the absorption

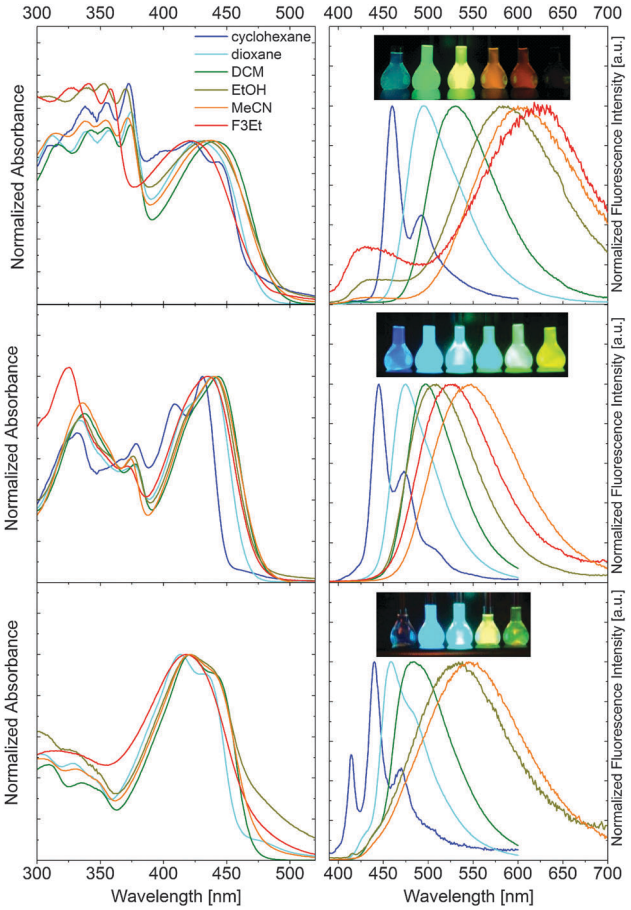

Fig. 3 Absorption and emission spectra of compound **2** (top), **3** (middle) and **4** (bottom) in different solvents. On the right, emission colours of these three cruciforms in the corresponding solvents (from left to right: cyclohexane, dioxane, DCM, EtOH, MeCN, F3Et).

spectra (depicted in Fig. 3 top), a clear ICT band appears at lower energies (420–450 nm), together with a band at around 370 nm that is attributed to the locally excited (LE) state. As the polarity of the solvent increases (Table 1, Fig. 3 top), this band shifts to longer wavelengths, except for protic solvents (EtOH and F3Et). The blue shift is likely attributed to specific solvent–solute interactions in these polar protic solvents, which should stabilize HOMO to a higher extent than the LUMO, since the former FMO has more density along the polar vertical axis. In fluorescence spectra, the emission band without vibrational resolution shifts dramatically to higher wavelengths, so that emission of this cruciforms covers practically the entire visible region as solvent polarity increases (Table 1, Fig. 3 top). As a consequence of strong electron-donating substitution in cruciform **2**, a much higher charge shift from the HOMO to the LUMO state is observed, relative to **1** (see ESI†). This ICT band is registered even after the excitation at the LE absorption, indicating a fast conversion from the LE to the ICT state. Indeed, similar quantum yields are obtained by exciting at LE (370 nm) or by directly pumping the ICT absorption band (at around 440 nm).

Generally, ICT transitions are characterized by high Stokes shifts and low fluorescence quantum yields in solvents with

high polarity. The main reasons for the low fluorescence efficiency under these conditions are: (*a*) the ICT state is so favoured (*i.e.* emits deeply in the red part of the spectrum) that the excited and the ground states are energetically very close, and the excited state deactivates mainly *via* non-radiative pathways, and/or (*b*) eventually the charge separation is so effective that a charge separated state (CS) evolves, which is non-emissive since the delocalized π-system is destroyed (the charges are localized).

However, in cruciform **2**, although the fluorescence efficiency is gradually reduced with the solvent polarity, the ICT emission is still relatively strong in the red part (605 nm) of the visible spectrum, showing ϕ = 0.26 in *e.g.* MeCN (Table 1). The two plausible reasons for this observed decrease in the efficiency of the non-radiative pathways are: (*a*) the inherent rigidity of the planar benzobisoxazole heretocycle core, and (*b*) the reduced flexibility of the chromophore in the excited state as a consequence of charge redistribution which converts the triple bond of the alkyne spacer (carbon atoms 15–17 and 16–18, see the ESI†) into an allenic fragment with two consecutive double bonds (carbon atoms 1–15 and 15–17, 4–16 and 16–18, see the ESI†). In contrast, ICT emission of compound **2** is quenched ($\phi_{fl} < 0.01$) at around 630 nm in F3Et, ascribed to the deactivation *via* non-radiative pathways in the red part and/or a CS promotion. Another possible reason could be the protonation of dimethylamino groups by this significantly acidic solvent. Indeed, the fluorescence decay of compound **2** in protic solvents does not follow mono-exponential kinetics, indicating the simultaneous contributions of several distinct species.

It is noteworthy to clarify this point. Generally, the two main factors that activate and stabilize the ICT are (*a*) the insertion of electron-donating and/or electron-accepting moieties, and (*b*) the polarity of the environment (solvent). Nonetheless, these conditions do not guarantee a high probability of an ICT emission, as too high a stabilization of the ICT can give rise to a red-edge emission but with a very reduced efficiency due to the higher influence of the non-radiative (k_{nr}) processes (above commented) under these conditions.[6]

For this reason, a good strategy to enhance fluorescence efficiencies in highly polar solvents is in fact to induce a less stabilized ICT transition. Thus, by the substitution of the strongly electron-donating 4-(*N*,*N*-dimethylamino)phenyl groups along the horizontal axis—previously identified as an electron-acceptor axis in **1**—in cruciform **3**, a more fluorescent ICT should be expected. First, note that the effect of the electron-donating group is strong enough to disrupt the inherent tendency of the vertical axis to bear the bulk of the HOMO density. In compound **3**, this trend is reversed: the HOMO is localized along the horizontal axis, and the LUMO is rather delocalized, but with somewhat higher density along the vertical axis (see the ESI† for images of individual FMOs). Indeed, the ionization potential of **3** is −7.95 eV, which is between the values for cruciforms **2** and **1**.

The absorption and fluorescence spectra of compound **3** are similar to those of **2**, but with a lower solvatochromic effect and higher fluorescence quantum yields (Fig. 3, middle; Table 1), which remain high even in polar media (*e.g.* in F3Et, $\phi_{fl} > 0.5$).

The substitution of both axes by the electron-releasing 4-(*N*,*N*-dimethylamino)phenyl groups in cruciform **4** should preserve the inherent FMO separation of benzobisoxazole cruciforms (HOMO along the vertical axis, LUMO along the horizontal axis). The contour maps of the HOMO and LUMO of compound **4** corroborate this statement (see ESI†). Indeed, the recorded absorption and fluorescence spectra in cruciform **4** (Fig. 3 bottom, Table 1) are similar to those of cruciforms with 4-(*N*,*N*-dimethylamino)phenyl substituents (compounds **2** and **3**). Note that the multiexponential kinetics obtained in the fluorescence decay curves for most of the solvents suggests a complicated photophysical process in the excited state involving several interconverting states (LE, ICT and even CS). ICT in compound **4** is less feasible than in **3** for solvents of low polarity (cyclohexane and dioxane), but its emission is greatly stabilized in solvents with higher polarity (EtOH and MeCN), indicating a high solvatochromic effect. Only in acidic F3Et solvent, the emission from ICT is totally quenched, similar to the case of compound **2**, suggesting once again a specific interaction with amino groups positioned along the vertical axis.

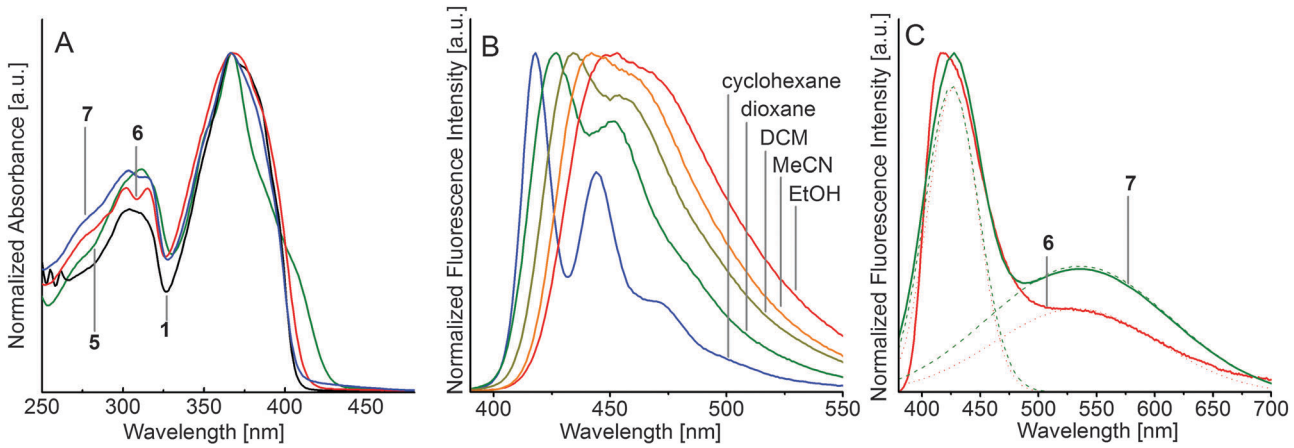

Fig. 4 (A) Height-normalized absorption spectra of compounds **5–7** and the reference compound **1** in DCM; (B) height-normalized emission spectra of compound **5** in different solvents, and (C) height-normalized emission spectra of compounds **6** and **7** in F3Et (deconvolution shown in dotted curves for **6** and dashed curves for **7**).

Next, we examined a series of three cruciforms with electron-poor 4-pyridyl group positioned either along the vertical or horizontal (or both) axes of the cruciforms. In the case of cruciform **5**, where the electron-withdrawing 4-pyridyl group is located along the inherently electron-poorer horizontal axis, the absorption spectra show the main band (LE) centred at a similar position to that in compound **1** but together with a shoulder at lower energies, which could be indicative of an ICT state operating in the ground state (Fig. 4A). On the other hand, the shape and position of the fluorescence spectra show a progressive change (Fig. 4B). With increasing polarity of the environment, the loss of vibrational resolution is apparent and is accompanied by a bathochromic shift leading to a much higher Stokes shift relative to compound **1** (Tables S1 and S2, ESI†)—confirming the ICT nature of the emission. However, it shows a much lower solvatochromic effect relative to the cruciforms bearing 4-(*N*,*N*-dimethylamino)phenyl groups, attributed to a lower charge transfer character in this system. That is because the electron-accepting character of the pyridine nucleus is apparently lower than the electron-releasing ability of the aniline. Indeed, the respective fluorescence quantum yields are high even in polar solvents (Table S2, ESI†) where the ICT emission dominates, in line with the lower charge transfer character of these derivatives.

For the cases of cruciforms with electron-withdrawing pyridine groups on the vertical axis, or along both horizontal and vertical axes (cruciforms **6** and **7**, respectively), absorption and emission spectra are very similar to those of the reference compound **1** (Fig. S1, Tables S3 and S4, ESI†) indicating negligible contributions from the ICT states. In fact, the substitution of the weakly electron-withdrawing pyridyl groups on both the horizontal and vertical axes of the cruciform does not produce any appreciable change in HOMO and LUMO states with respect to compound **1** (see the contour map in the ESI†), reflecting a very mild effect of the pyridyl substitution. Nevertheless, it is worth noting here the surprising behaviour of cruciforms **6** and **7** in F3Et: both show a dual emission attributed to the LE (at 440 nm) and ICT states (at around 540 nm, Fig. 4C). The formation of this ICT state could be due to the protonation of nitrogen of the pyridyl group on the vertical axis, which would greatly increase the acceptor ability since the pyridinium group is a stronger electron-withdrawing group. The dual emission covering a wide region of the visible spectra (400–650 nm) with a relatively high quantum yields (ϕ_{fl} = 0.35 to 0.40) is an interesting feature to be used for white light production upon UV excitation.

Finally, we studied the photophysical properties of cruciforms with the combination of both electron-donating 4-(*N*,*N*-dimethylamino)phenyl and electron-withdrawing 4-pyridyl groups. In compound **8**, the aniline groups are positioned on the vertical axis and the 4-pyridyl groups along the horizontal axis, enhancing the inherent tendency of this kind of cruciforms to localize the HOMO along the vertical axis, and LUMO along the horizontal one. Hence, the intramolecular charge transfer process should be the one with the highest charge separation and accordingly the highest probability of ICT formation. Indeed, a very red-shifted ICT emission with high fluorescence quantum yield is dominating already in solvents

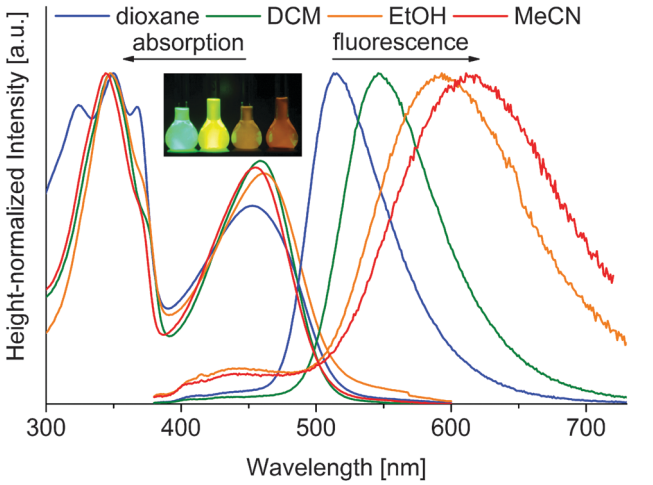

Fig. 5 Height-normalized absorption and emission spectra of compound **9** in different solvents. Inset: a photograph of emission colors of compound **9** in dioxane, DCM, EtOH, and MECN (from left to right) under UV light (λ_{exc} = 360 nm).

of low polarity (Table 1; Fig. S2, ESI†). However, the stabilization of the ICT by the further increase in solvent polarity results in total quenching of the emission signal, presumably because greater stabilization of an ICT state in the red part of the spectrum leads to dominant non-radiative relaxation (or even the formation of a dark CS state).

In this sense, an increase in quantum yield in polar solvents can be expected if the strong electron-donor 4-(*N*,*N*-dimethylamino)-phenyl is substituted along the electron-accepting horizontal axis and weak electron-acceptor (pyridine) positioned along the inherently electron-donating vertical axis, as in cruciform **9**. In this case, the electronic behaviour of the axis is inverted, with the HOMO localized along the horizontal axis, and LUMO along the vertical axis (see ESI†). Accordingly, the ICT character of compound **9** is attenuated relative to its analogue **8**, but more favoured than in compounds **2**–**4**. It shows a strong bathochromic shift with the solvent polarity reaching the red emission part (Fig. 5) with quantum yields higher than 0.20 (Table 1).

In summary, we have studied the photophysical behavior of nine cruciforms where fluorescent ICT transition can be activated to a different extent by electron-donating 4-(*N*,*N*-dimethylamino)-phenyl or electron-withdrawing 4-pyridyl groups, which can be positioned pairwise along the vertical or horizontal axes. Fig. 6 clearly shows how different is the stabilization of ICT excited states in DCM depending on the substitution patterns in the cruciform. The emission colour can be modulated from blue in the poorly activated ICT with the electron-withdrawing 4-pyridyl groups on the horizontal axis (compound **5**) to red in the most favourable ICT formation, caused by the insertions of electron-withdrawing 4-(*N*,*N*-dimethylamino)phenyl groups along the vertical axis and the electron-withdrawing 4-pyridyl groups on the horizontal axis (compound **8**). Thanks to the inherently polar nature of ICT transition, emission can also be modulated by the characteristics of the environment. Therefore, most of these fluorophores should work very well as fluorescence polarity sensors on the basis of the variable stabilization of the ICT state by different solvents.

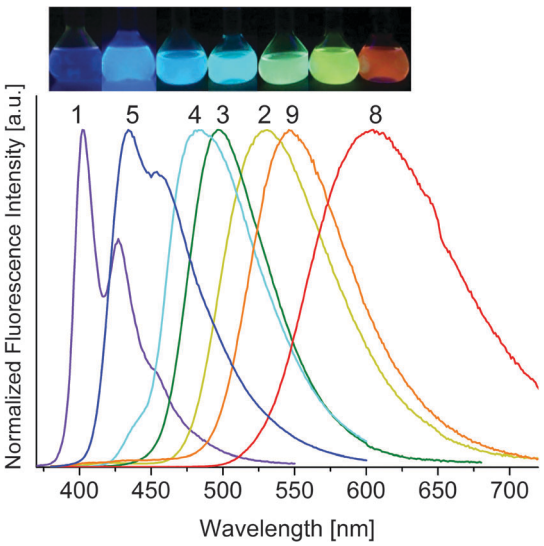

Fig. 6 Height-normalized ICT emission spectra of compounds **1–5**, **8** and **9** in DCM.

Conclusions

All the compounds with the electron-donating 4-(*N*,*N*-dimethylamino)phenyl group (**2–4**, **8** and **9**) show ICT states even in the ground state. The influence of this substituent is the highest when incorporated along the vertical axis, where it augments the inherent tendency of bis(ethynyl)benzobisoxazole cruciforms to localize the HOMO along the vertical axis. On the other hand, the substitution with the electron-withdrawing 4-pyridyl group (compounds **5–7**) is not sufficient to induce CT in the ground state; only when it is placed along the preferred electron-accepting horizontal axis can a poorly activated ICT emission be detected. Along the same lines, the strongest solvatochromism effect is found for the cruciform substituted with the electron-donating 4-(*N*,*N*-dimethylamino)phenyl group on the vertical axis and the electron-withdrawing 4-pyridyl group on the horizontal axis.

Except in those cases where the ICT transition is too activated and the emission bands are shifted deeply into the red region, the fluorescence quantum yields of most ICT emissions in these cruciforms are relatively high even in polar solvents ($\phi > 0.2$). This fact is attributed to the planarity and high rigidity of the benzobisoxazole heterocyclic core and the change of the triple bond in acetylene spacer (in HOMO) to an allene motif (in LUMO) after the excitation, which gives rise to a rigid chromophore and decreases the likelihood of non-radiative relaxation pathways.

Thus, ICT transitions can be modulated by the insertion of different substituents (moderately electron-withdrawing 4-pyridyl and/or strongly electron-donating 4-(*N*,*N*-dimethylamino)phenyl groups) in different positions of the cruciform (horizontal and/or vertical axis) offering the choice of emission colours that essentially spans the entire visible range. These cruciforms could therefore be used as solvent polarity indicators that can cover a broad solvatochromic range based on their substitution pattern.

Acknowledgements

This work was funded by the Gobierno Vasco (IT 339-10), the Welch Foundation (award E-1768), the US National Science Foundation (award CHE-1151292) and the University of Houston. V.M.M. acknowledges Ministerio de Economía y Competitividad (MINECCO) for Ramón y Cajal (RYC-2011-09505) fellowship. O.Š.M. is a Cottrell Scholar of the Research Foundation for Science Advancement.

Notes and references

1 (*a*) A. J. Zucchero, P. L. McGrier and U. H. F. Bunz, *Acc. Chem. Res.*, 2010, **43**, 397–408; (*b*) A. K. Feldman, M. L. Steigerwald, X. Guo and C. Nuckolls, *Acc. Chem. Res.*, 2008, **41**, 1731–1741.

2 (*a*) K. Ohta, S. Yamada, K. Kamada, A. D. Slepkov, F. A. Hegmann, R. R. Tykwinski, L. D. Shirtcliff, M. M. Haley, P. Sałek, F. Gel'mukhanov and H. Ågren, *J. Phys. Chem. A*, 2011, **115**, 105–117; (*b*) C. N. Carroll, J. J. Naleway, M. M. Haley and D. W. Johnson, *Chem. Soc. Rev.*, 2010, **39**, 3875–3888; (*c*) E. L. Spitler and M. M. Haley, *Tetrahedron*, 2008, **64**, 11469–11474; (*d*) E. L. Spitler, J. M. Monson and M. M. Haley, *J. Org. Chem.*, 2008, **73**, 2211–2223; (*e*) E. L. Spitler, L. D. Shirtcliff and M. M. Haley, *J. Org. Chem.*, 2007, **72**, 86–96; (*f*) A. Bhaskar, R. Guda, M. M. Haley and T. Goodson III, *J. Am. Chem. Soc.*, 2006, **128**, 13972–13973; (*g*) J. A. Marsden, J. J. Miller, L. D. Shirtcliff and M. M. Haley, *J. Am. Chem. Soc.*, 2005, **127**, 2464–2476; (*h*) J. J. Miller, J. A. Marsden and M. M. Haley, *Synlett*, 2004, 165–168.

3 (*a*) T. Schwaebel, O. Trapp and U. H. F. Bunz, *Chem. Sci.*, 2013, **4**, 273–281; (*b*) J. Kumpf and U. H. F. Bunz, *Chem.–Eur. J.*, 2012, **18**, 8921–8924; (*c*) C. Patze, K. Broedner, F. Rominger, O. Trapp and U. H. F. Bunz, *Chem.–Eur. J.*, 2011, **17**, 13720–13725; (*d*) M. N. Gard, A. J. Zucchero, G. Kuzmanich, C. Oelsner, D. Guldi, A. Dreuw, U. H. F. Bunz and M. A. Garcia-Garibay, *Org. Lett.*, 2012, **14**, 1000–1003; (*e*) E. A. Davey, A. J. Zucchero, O. Trapp and U. H. F. Bunz, *J. Am. Chem. Soc.*, 2011, **133**, 7716–7718; (*f*) P. L. McGrier, K. M. Solntsev, A. J. Zucchero, O. R. Miranda, V. M. Rotello, L. M. Tolbert and U. H. F. Bunz, *Chem.–Eur. J.*, 2011, **17**, 3112–3119; (*g*) J. Tolosa, K. M. Solntsev, L. M. Tolbert and U. H. F. Bunz, *J. Org. Chem.*, 2010, **75**, 523–534; (*h*) A. J. Zucchero, R. A. Shiels, P. L. McGrier, M. A. To, C. W. Jones and U. H. F. Bunz, *Chem.–Asian J.*, 2009, **4**, 262–269; (*i*) J. Tolosa and U. H. F. Bunz, *Chem.–Asian J.*, 2009, **4**, 270–276; (*j*) P. L. McGrier, K. M. Solntsev, S. Miao, L. M. Tolbert, O. R. Miranda, V. M. Rotello and U. H. F. Bunz, *Chem.–Eur. J.*, 2008, **14**, 4503–4510; (*k*) J. Tolosa, A. J. Zucchero and U. H. F. Bunz, *J. Am. Chem. Soc.*, 2008, **130**, 6498–6506; (*l*) S. M. Brombosz, A. J. Zucchero, R. L. Phillips, D. Vasquez, A. Wilson and U. H. F. Bunz, *Org. Lett.*, 2007, **9**, 4519–4522; (*m*) M. Hauck, J. Schönhaber, A. J. Zucchero, K. I. Hardcastle, T. J. J. Müller and U. H. F. Bunz, *J. Org. Chem.*, 2007, **72**, 6714–6725; (*n*) P. L. McGrier, K. M. Solntsev,

J. Schönhaber, S. M. Brombosz, L. M. Tolbert and U. H. F. Bunz, *Chem. Commun.*, 2007, 2127–2129; (*o*) A. J. Zucchero, J. N. Wilson and U. H. F. Bunz, *J. Am. Chem. Soc.*, 2006, **128**, 11872–11881; (*p*) W. W. Gerhardt, A. J. Zucchero, J. N. Wilson, C. R. South, U. H. F. Bunz and M. Weck, *Chem. Commun.*, 2006, 2141–2143; (*q*) J. N. Wilson and U. H. F. Bunz, *J. Am. Chem. Soc.*, 2005, **127**, 4124–4125; (*r*) J. N. Wilson, M. D. Smith, V. Enkelmann and U. H. F. Bunz, *Chem. Commun.*, 2004, 1700–1701; (*s*) J. N. Wilson, K. I. Hardcastle, M. Josowicz and U. H. F. Bunz, *Tetrahedron*, 2004, **60**, 7157–7167; (*t*) J. N. Wilson, M. Josowicz, Y. Wang and U. H. F. Bunz, *Chem. Commun.*, 2003, 2962–2963.

4 (*a*) M. Jo, J. Lim and O. Š. Miljanić, *Org. Lett.*, 2013, **15**, 3518–3521; (*b*) J. Lim and O. Š. Miljanić, *Chem. Commun.*, 2012, **48**, 10301–10303; (*c*) J. Lim, D. Nam and O. Š. Miljanić, *Chem. Sci.*, 2012, **3**, 559–563; (*d*) J. Lim, T. A. Albright, B. R. Martin and O. Š. Miljanić, *J. Org. Chem.*, 2011, **76**, 10207–10209; (*e*) J. Lim, K. Osowska, J. A. Armitage, B. R. Martin and O. Š. Miljanić, *CrystEngComm*, 2012, **14**, 6152–6162; (*f*) K. Osowska and O. Š. Miljanić, *Chem. Commun.*, 2010, **46**, 4276–4278. For related benzimidazole-based fluorophores, see: (*g*) R. C. Lirag, H. T. M. Le and O. Š. Miljanić, *Chem. Commun.*, 2013, **49**, 4304–4306.

5 (*a*) Y. Marcus, *Chem. Soc. Rev.*, 1993, **22**, 409–416; (*b*) J. Catalán, *J. Phys. Chem. B*, 2009, **113**, 5951–5960.

6 Z. R. Grabowski, K. Rotkiewicz and W. Rettig, *Chem. Rev.*, 2003, **103**, 3899–4031.